A Boundary Stress Model for Fillet-Welded Connection Plates

LOGAN CALLELE

ABSTRACT

A common structural steel connection design problem is to size a fillet-welded plate boundary for an eccentric shear and/or normal force. Three common design models for dealing with the design of the fillet-welded plate boundary are reviewed, and a new model is presented. The new model is derived to produce designs similar to the instantaneous center of rotation method; however, the model offers an explicit solution by assuming a stress distribution on the boundary that designers can easily confirm or modify in daily practice.

Keywords: fillet weld, instantaneous center of rotation, welded connection, plate boundary, eccentric shear.

INTRODUCTION

The design of steel connections typically involves the following steps:

1. Discussion with the steel fabricator and erector on the preferred connection types, appropriate to the type and magnitude of the structural loading, that promote efficient fabrication and construction.
2. Assess the selected connection's geometry at the various joint types.
3. Draw a free-body diagram of the joint, and make the necessary assumptions on the load path. A clear understanding of the assumed load path is especially important for evaluating transfer forces or when portions of the load pass through multiple connection elements.
4. Perform design checks on the connection elements to ensure that suitable plates, welds, bolts and (if required) reinforcement are provided to transfer the forces from step 3.

One of the basic connection elements is the fillet-welded plate that has an eccentric shear force applied; see Figure 1 for just a few of the many possible examples. The implication of the eccentric shear is that the fillet weld will need to transfer a transverse shear stress, where "transverse" refers to the orientation of the direction of the shear stress with respect to the long axis of the fillet weld. Depending on the design assumptions, it is also common to have to transfer a normal force across the fillet-welded boundary of the connection plate; a schematic representation of this is shown in Figure 2.

This paper will review three common design models for designing the fillet-welded plate boundary to account for an eccentric shear and normal force, and a new model will be presented. The new model will be shown to give designs that match the instantaneous center of rotation method, which forms the basis of Table 8-4 of the AISC *Steel Construction Manual*, hereafter referred to as the AISC *Manual* (2011). However, the new method can easily be expanded to other scenarios that Table 8-4 does not cover and allows the designer to follow the load path of the assumed boundary stress on the connection plate into the member that the plate is welded to. As an example, the connection plates shown in Figure 1 are welded to W-shape steel sections, and local web strength and stability may limit the stress that can be transferred across the boundary. The proposed new model will allow the designer to follow the assumed load path across the welded boundary of the connection plate and assess any potential impacts of local yielding or crippling of the W shape web while still accounting for the load-deformation and ductility characteristics of the fillet weld.

Design Model 1—Elastic Stress Distribution

A common design approach is to apply a linear elastic stress distribution (Blodgett, 1966), see Figure 3, to the transverse shear stress of the fillet-welded boundary of the connection plate. This results in a maximum transverse shear, σ_M, as given in Equation 1:

$$\sigma_M = \frac{P}{H} + 6\frac{Ve}{H^2} \quad (1)$$

The critical stress at the end of the plate, σ_M, is vectorially

Logan Callele, M.Sc., P. Eng., Engineering Manager, Waiward Steel, Edmonton, Alberta, Canada. Email: logan.callele@waiward.com

Paper No. 2015-18R

combined with the applied longitudinal shear stress on the fillet weld to allow the designer to determine the required fillet weld size for the applied loading. This size is calculated by setting the design strength of the fillet weld, as defined by Equation J2-5 of the AISC *Specification for Structural Steel Buildings*, hereafter referred to as the AISC *Specification*, equal to the critical stress at the end of the plate (AISC, 2010). This method is conservative and easily calculated; however it can result in excessive welding, plate sizes, and joint reinforcing—increasing the cost of the fabricated steel.

Design Model 2—Plastic Stress Distribution

Another common approach is to use a plastic stress distribution (Muir and Thornton, 2014), also shown in Figure 3, where a limiting stress, σ_P, is assessed—($F_y \times t$) for plate design, for example—and the behavior of the connection component is assumed to have enough ductility to allow the full length of the plate to reach the stress state corresponding to σ_P prior to rupture. The resulting nominal moment is given in Equation 2:

$$M_n = \frac{\sigma_P}{4}\left[H^2 - \left(\frac{P}{\sigma_P}\right)^2\right] \tag{2}$$

The advantages to the plastic approach are that it is easily calculated and it allows greater connection efficiency than Design Model 1 by using the maximum possible capacity for the connection component. The disadvantage to the plastic

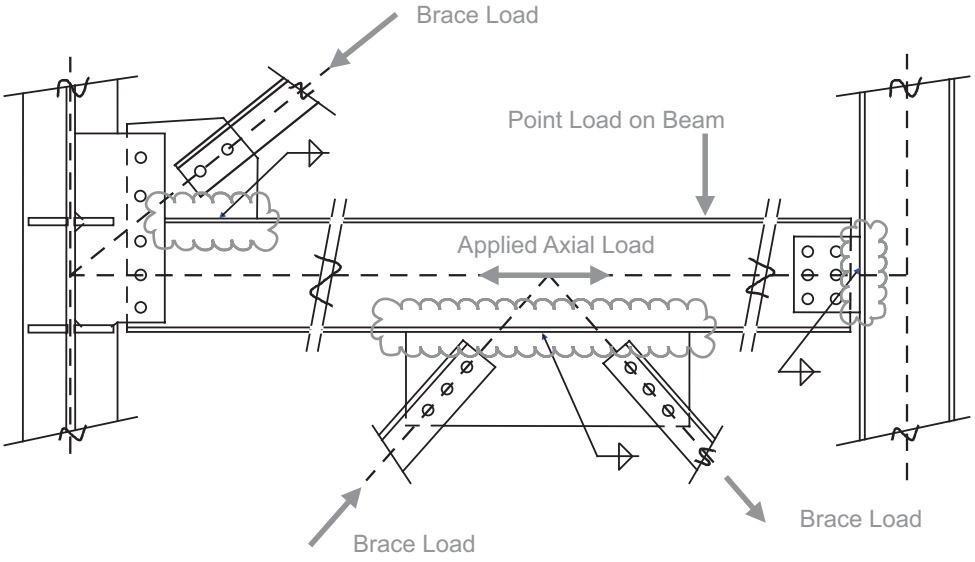

Fig. 1. Fillet-welded connection plate elements under eccentric shear.

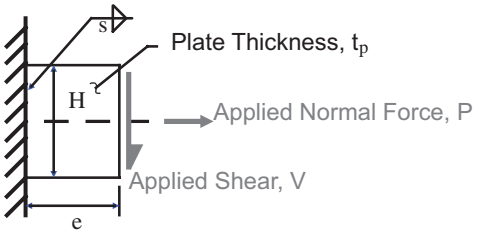

Fig. 2. Schematic of a fillet-welded connection plate loaded with eccentric shear and a concentric normal force.

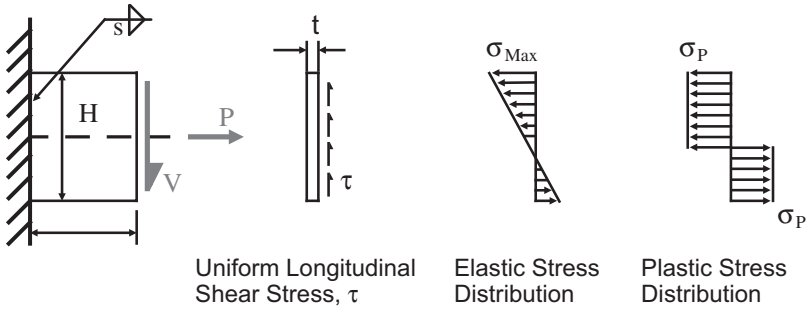

Fig. 3. Assumed stress distributions for Design Models 1 and 2.

approach is that it only evaluates the capacity of the connection, and therefore defining a stress state under a given load is not easy. The designer must also ensure that there is sufficient ductility to allow the critical stress σ_P to be reached across the full length of the connection element. One common approach to ensuring sufficient ductility across a connection boundary is the "Richards" or "ductility" factor discussed by Hewitt and Thornton (2004), which allows the designer to evaluate a peak stress along the length of the connection and ensure that this peak stress does not cause premature failure of the welds.

Design Model 3—Instantaneous Center of Rotation

The instantaneous center of rotation (ICoR) approach for the design of eccentrically loaded fillet welds has been in use for more than 40 years (Butler et al., 1972). Because it has been discussed in detail in numerous other publications, it will not be described in detail here. The ICoR analysis is a rational approach that assumes rigid-body rotation of the plate and accounts for the measured strength and ductility characteristics of fillet welds. It provides good agreement with tested capacities of fillet welds under eccentric shear (Lesik and Kennedy, 1990), and through the use of tabulated *C* values found in design handbooks, such as Table 8-4 of the AISC *Manual* (AISC, 2011), the numerical iterations required by the method are eliminated for design purposes. However, the designer is required to use the assumed connection geometry and loading assumptions used in generating the tabulated *C* values or interpolate between tabulated values. Also, there is no direct way to follow the load path across the boundary and assess if local web strength or stability limit states may reduce the magnitude of eccentric shear that can be applied to the connection element.

Design Model 4—Proposed New Model: Elliptical Stress Distribution

One other drawback to Design Model 3 is that the assumed stress distribution is not explicitly given, as would be the case when Design Models 1 or 2 are used. Thus, the development of Design Model 4 will start with a qualitative evaluation of the assumed stress distribution resulting from a typical ICoR analysis.

The ICoR method is performed herein with the weld characteristics described in Callele et al. (2009), which are summarized in Figure 4 and in the following equations:

$$\frac{F}{R_n} = \left[\rho(2-\rho)\right]^{0.25} \text{ if } \rho \geq 0.07a \tag{3}$$

$$\frac{F}{R_n} = 8.7\rho \text{ if } \rho < 0.07 \tag{4}$$

$$\rho = \frac{\Delta}{\Delta_{ult}} \tag{5}$$

$$\frac{\Delta_{ult}}{s(\sin\theta + \cos\theta)} = 0.2(\theta + 2)^{-0.36} \tag{6}$$

In Equations 3 and 4, R_n is the nominal strength of the fillet weld, as given by Equation J2-5 of the AISC *Specification* (AISC, 2010). In Equation 5, is the fillet weld deformation in the direction of the applied load, *F*. The deformation of the fillet weld when it reaches its maximum stress—that is, its nominal strength—is Δ_{ult}.

The ICoR analysis is performed assuming that dividing the weld length along the plate height into 50 discrete segments would provide sufficient accuracy. Also, the ICoR analysis only allows the critical fillet-weld segment(s) deformation to reach Δ_{ult}. Thus, at the available strength of the weld, as calculated by the ICoR used herein, the critical weld segment(s) has(have) reached its (their) maximum stress but not its (their) maximum deformation capacity.

In order to confirm that the ICoR analysis was correctly applied the *C* values shown in Table 8-4 of the AISC *Manual* were calculated for θ = 0°, 15°, 30°, 45°, 60° and 75°. These values are shown and compared in Tables 1 through 6 and the average percent difference between the *C* values provided in Table 8-4 and the ICoR analysis is 0.1%, which is considered acceptable to prove the validity of the author's ICoR analysis. The small discrepancy reflects slightly different weld properties assumed and convergence criteria used in evaluating the *C* values shown in Table 8-4.

Figures 5 and 6, respectively, plot the transverse and longitudinal fillet weld shear stress distributions resulting from an ICoR analysis of the following situation, with reference to Figure 2: P = 50 kips, s = 5/16 in., H = 16 in., and e = 8 in. The figures give a qualitative assessment of the typical stress distribution resulting from the deformation and compatibility assumptions of the ICoR analysis.

The distribution of transverse stress along the plate height is shown to be nonlinear in Figure 5. Various nonlinear

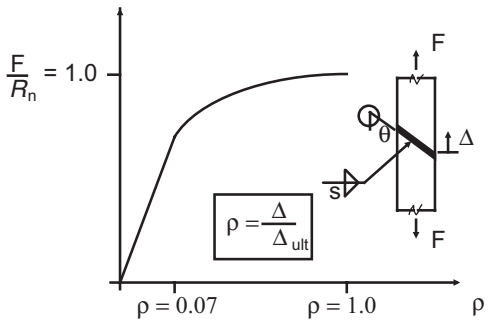

Fig. 4. Assumed fillet weld load deformation behavior for instantaneous center of rotation analysis.

functions were evaluated, and the elliptical approximation of the transverse stress shown in Figure 5 was found to give the best agreement with the distribution of the fillet weld's transverse shear stress. The elliptical distribution is scaled so that the neutral axis and maximum transverse shear stress at the end of the weld length form the apexes of the ellipse. It is worth noting that the load-deformation response curve assumed for the fillet weld has an elliptical form as well, as shown in Equation 3.

In Figure 6, the distribution of the fillet weld longitudinal shear stress, from the ICoR example, is also seen to be nonlinear over the height of the plate. This is an interesting observation as Design Models 1 and 2 typically assume a uniform distribution of longitudinal shear stress, but it is consistent with the nonuniform shear stress distribution on a rectangular cross-section under flexure that would be obtained with classic elastic analysis. However, assuming a uniform distribution of shear stress, the critical weld segment at the end of the weld will then have a larger longitudinal shear stress than the same critical elements analyzed with the ICoR approach. The assumed larger longitudinal shear stress at the ends will result in a smaller transverse shear stress on the critical elements. Thus, the assumption of uniform distribution of the longitudinal shear will be used for Design Model 4 for ease of calculation and because it is a conservative assumption.

Given the reasonable qualitative agreement of the elliptical distribution shown in Figure 5, Design Model 4 will be developed in a manner similar to Design Model 2 but with an assumed elliptical transverse shear stress distribution. Design Model 4 will allow the designer to address the design of the boundary as a whole, rather than solely focusing on the fillet welds, though it accounts for the strength and ductility behavior of welds. It will be developed so that the designer directly accounts for any local web yielding or crippling at the boundary of the connection plate that may limit the available strength of the connection, ensuring that all limit states are checked and are consistent with the model's assumptions.

DERIVATION OF DESIGN MODEL 4

The proposed model uses an assumed elliptical transverse shear stress distribution that is qualitatively similar to the resulting stress distribution from an ICoR analysis. As previously discussed, Design Model 4 will be developed

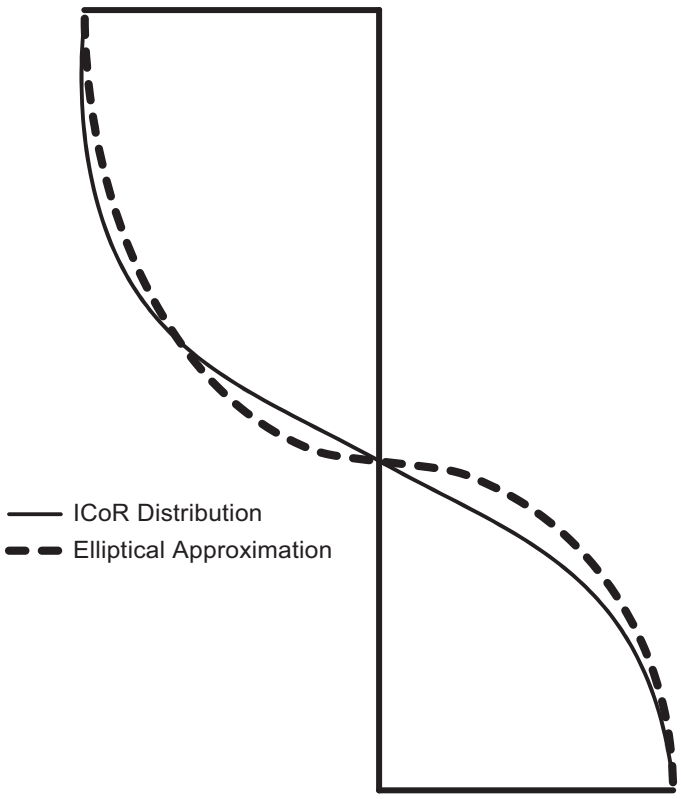

Fig. 5. ICoR transverse shear stress distribution on paired eccentrically loaded fillet weld.

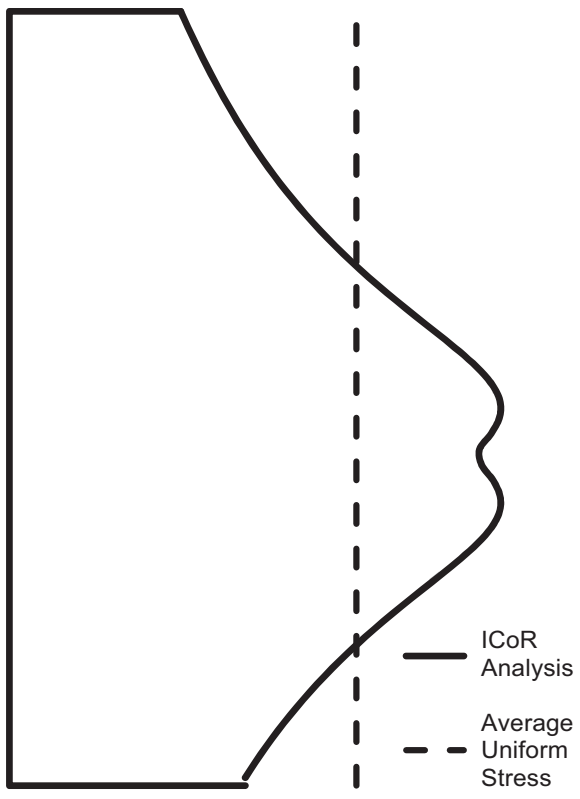

Fig. 6. ICoR longitudinal shear stress distribution on paired eccentrically loaded fillet weld.

assuming that the longitudinal shear stress is uniformly distributed along the length of the connection. Lastly, the model will be developed to allow for two different possibilities: the first assuming no plate bearing and the second assuming that the plate does go into bearing. Note that it is a conservative assumption, and consistent with Table 8-4 of the AISC *Manual* (AISC, 2011), to assume that plate bearing does not occur.

With reference to Figure 7, which shows a schematic of the assumed stress distribution for Design Model 4 with no plate bearing, the longitudinal shear stress, τ, is defined as:

$$\tau = \frac{V}{H} \tag{7}$$

Using a similar procedure to the classical derivation of Design Model 2, the neutral axis position, shown as y in Figure 7, is evaluated in Equation 8 by equilibrating the transverse shear stress distribution with the applied normal force, P, and using the properties of a quarter ellipse—a quarter ellipse of height a and width b has an area of $\frac{\pi ab}{4}$ and a centroid that is $\frac{4a}{3\pi}$ away from side b. The resulting expression for the nominal moment strength of the weld group is shown in Equation 9. See Appendix A and Figure 8 for more details about the derivation of Equations 8 and 9.

$$y = \frac{H}{2} - \frac{2P}{\pi \sigma_T} \tag{8}$$

$$M_n = \sigma_T \left(\frac{\pi}{4} - \frac{1}{3} \right) \left[y^2 + (H - y)^2 \right] - P \left(\frac{H}{2} - y \right) \tag{9}$$

If the connection plate is welded to a W-shape flange, the designer can now follow the assumed load path by ensuring that the resultant compressive force, F_c, from the assumed elliptical stress distribution does not exceed the local web yielding and/or crippling limit states given in Sections J10.2 through J10.5 of the AISC *Specification* (AISC, 2010). The magnitude of the compressive force, F_c, is shown in Equation 10:

$$F_c = \frac{\pi}{4} (\sigma_T y) \tag{10}$$

There are two steps remaining to complete Design Model 4. The first step calculates the fillet weld strength used in this model, σ_T; note that σ_T has units of force per unit length. The second step shows the adjustment to the model should the compressive force, F_c, exceed the web design strength or stability limitations of the W-shape that the connection plate is welded to.

Evaluation of Fillet Weld Strength, σ_T

The maximum transverse shear stress on a fillet weld under a given longitudinal shear stress is the critical stress, σ_T, that must be calculated. When vectorially added, the critical stress, σ_T, and the corresponding longitudinal stress, τ, represent the fillet weld's nominal strength. The strength of fillet welds under concentric loading, V_n, has been discussed in detail (e.g., see Lesik and Kennedy, 1990) and is given in the AISC *Specification* (AISC, 2010), Equation J2-5, as shown in Equation 11; note that the design strength of the weld in LRFD is ϕV_n with $\phi = 0.75$:

$$V_n = 0.6 A_w F_{EXX} \left(1.0 + 0.5 \sin^{1.5} \theta \right) \tag{11}$$

There is a difficulty in directly using Equation 11 to establish σ_T, though; the load angle, θ, the tangent of which is defined as the ratio of the transverse shear to the longitudinal shear, is not explicitly known. However, Equation 11 can be reworked to provide a strength criterion that allows the explicit definition of the transverse and longitudinal components of the stress applied to fillet welds by splitting the nominal weld strength as given in Equation 11 into the following:

$$V_n = \sqrt{{V_{nL}}^2 + {V_{nT}}^2} \tag{12}$$

$$V_{nL} = 0.6 A_w F_{EXX} N_L \tag{13}$$

$$V_{nT} = 0.6 A_w F_{EXX} N_T \tag{14}$$

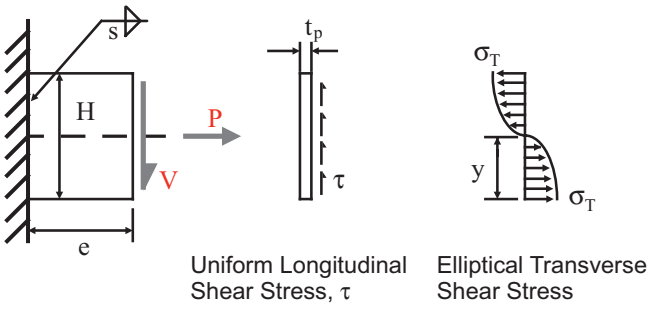

Fig. 7. Assumed stress distribution for Design Model 4—no plate bearing.

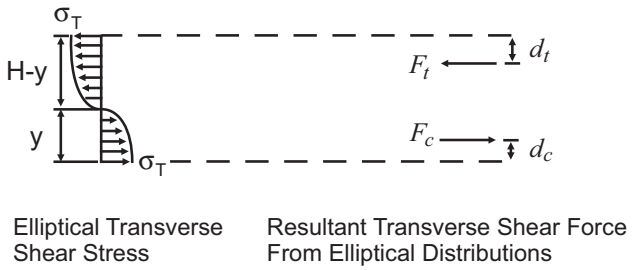

Fig. 8. Resultant forces from assumed stress distribution.

The values N_L and N_T are defined as the ratio of the applied load, in the respective longitudinal and transverse directions, to the fillet weld nominal strength with no consideration for the increase in strength with increasing value of θ—that is, $0.6A_wF_{EXX}$. The relationships between N_L and N_T and θ are given in Equations 15 and 16, but the following constraints also apply: $0 \le N_L \le 1.0$ and $0 \le N_T \le 1.5$.

$$\text{When } N_T \ge 0.6, \left(\frac{N_T - 0.6}{0.9}\right)^2 + N_L^2 = 1.0 \tag{15}$$

$$\tan\theta = \frac{N_T}{N_L} \tag{16}$$

Equation 15 is an elliptical equation, similar in form to the von Mises failure criterion, and it is plotted and compared with Equation 11 in Figure 9. The comparison is seen to be good, and the average difference between the two is less than 5%. Thus, the failure criteria given by Equation 15 is simply a different way of stating the well-established fillet weld strength criterion given in Equation 11 that has been used for more than 20 years. Equation 15 can be useful for designers when they must establish the maximum transverse shear stress allowable on a fillet weld under a given longitudinal shear stress, or vice versa, such that the stress applied to the weld metal is equal to the nominal strength of the fillet weld.

It is seen that in Figure 9, the value of N_L calculated by Equation 11 can be larger than 1.0 for values of $N_T \le 0.686$. This means that if a weld was first loaded to its capacity in longitudinal shear and then a transverse shear was applied, the weld's predicted longitudinal shear strength would increase (though it is relatively small—approximately a 3% maximum increase). This slight increase is ignored in Equation 15 and is why the elliptical failure equation is only applied after $N_T > 0.6$—that is, if $N_T \le 0.6$, then $N_L = 1.0$.

Using Equation 15, σ_T can now be evaluated as follows:

$$N_L = \frac{\tau}{0.6s\sqrt{2}F_{EXX}} \tag{17}$$

Then, if $N_L = 1.0$, use $N_T = 0.6$, and while N_T could safely be taken as any value between 0 and 0.6, a value of 0.6 is used, which corresponds to $\theta \cong 31°$, to maximize the design strength of the fillet weld. When $N_L < 1.0$, use Equation 18 to calculate N_T, after which Equation 19 can be used to calculate σ_T. In Equation 19, s is the fillet weld leg size, as shown in Figure 2.

$$N_T = 0.6 + 0.9\sqrt{1.0 - N_L^2} \tag{18}$$

$$\sigma_T = 0.6\sqrt{2}sF_{EXX}N_T \tag{19}$$

When designing with LRFD, Equations 17 and 19 would be modified by applying a value for $\phi = 0.75$ as follows: in Equation 17, define τ with an applied factored force and multiply the denominator by ϕ. Equation 19 must also be multiplied by ϕ and then used with Equations 8 and 9 to calculate the fillet weld design strength, which is to be compared to the applied factored eccentric force, *Ve*.

Modification of Design Model 4 to Account for Web Strength and Stability Limit States

Should the compressive force, F_c, given in Equation 10, exceed the design strength of any of the applicable web strength or stability limit states, given in Section J10 of the

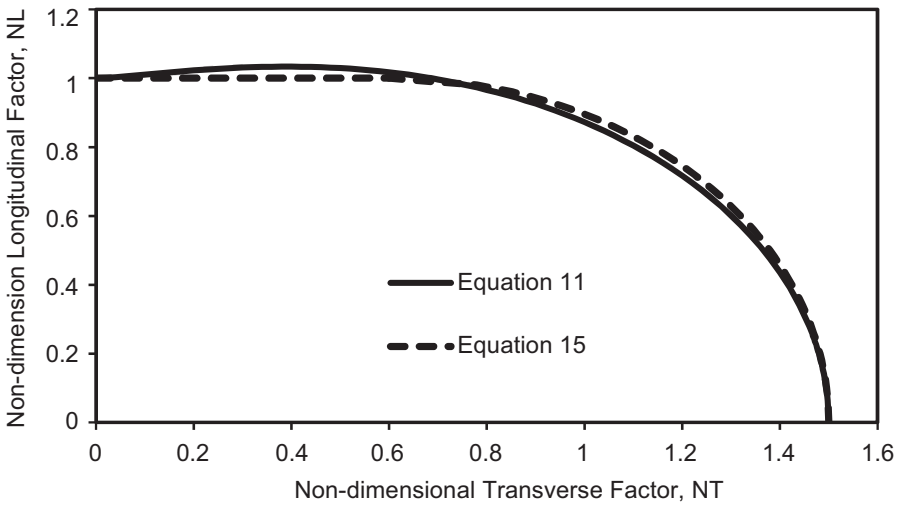

Fig. 9. Alternate elliptical fillet weld failure criteria compared to AISC Specification Equation J2-5.

Specification (AISC, 2010), then the assumed stress distribution and value of σ_T cannot be developed. In order to adjust the stress distribution to ensure the assumed boundary stresses do not exceed any local limit states in the W-shape, the elliptical stress distribution will be modified to assume plate bearing, and the bearing force will be limited to a value that satisfies the web limit states. The developed model will also be used in comparisons with test results from various research programs that had eccentrically loaded, fillet-welded connection plates specifically fabricated to ensure that the plate was in bearing.

When checking Equation 10 against the available strengths determined using Section J10 of the AISC *Specification*, the bearing length, l_b, is calculated using Equation 20. This equation ensures that the line of action of the resultant forces from the assumed elliptical stress distribution and the web resistance are aligned; see Figure 16 and Design Example 2 for more information.

$$l_b = 2\left(\frac{4\sigma_T}{3\pi}\right) \tag{20}$$

To account for bearing, either a triangular or rectangular stress distribution in the bearing region is typically considered; see Kwan et al. (2010). With reference to Figure 10, which shows a triangular bearing stress distribution, and applying a similar method as before, the resulting location of the neutral axis and nominal flexural strength of the welded boundary is given in Equations 21 and 22, respectively. Note that Equation 7 still applies to quantify the assumed uniform longitudinal shear stress distribution.

$$y = \frac{\frac{\pi}{4}(\sigma_T H) - P}{\frac{\pi}{4}\sigma_T + \frac{\sigma_{Br}}{2}} \tag{21}$$

$$M_n = \sigma_T\left(\frac{\pi}{4} - \frac{1}{3}\right)(H-y)^2 + \frac{\sigma_{Br}y^2}{3} - P\left(\frac{H}{2} - y\right) \tag{22}$$

The assumed value for σ_{Br} that the author feels is appropriate is the governing yield stress of either the plate or the W-shape web—the critical value of σ_{Br}—and is given in Equation 23:

$$\sigma_{Br} = Min\begin{vmatrix} F_{yp} \times t_p \\ F_{yw} \times t_w \end{vmatrix} \tag{23}$$

By using Equation 23, the local web yielding will be satisfied in the W-shape, and if local crippling governs the length of the triangular stress, the block may need to be adjusted so that the resultant bearing force satisfies the crippling limit state. To be consistent with Section J10.2 of the AISC *Specification*, use $\phi = 1.0$ with Equation 23 to obtain the design strength when using LRFD.

If the designer wanted to consider a rectangular stress block for the bearing, Equations 21 and 22 could be modified as follows:

$$y = \frac{\frac{\pi}{4}(\sigma_T H) - P}{\frac{\pi}{4}\sigma_T + \sigma_{Br}} \tag{24}$$

$$M_n = \sigma_T\left(\frac{\pi}{4} - \frac{1}{3}\right)(H-y)^2 + \frac{\sigma_{Br}y^2}{2} - P\left(\frac{H}{2} - y\right) \tag{25}$$

COMPARISON OF DESIGN MODELS AND DISCUSSION

Equation 9 represents the nominal strength of the fillet-welded boundary when an eccentric shear is applied as shown in Figure 2. Using LRFD, if the design strength is greater than or equal to the moment resulting from the factored eccentric shear, *Ve*, the weld design will be considered adequate. It is seen that Equation 9 is similar in form to the classical elastic and plastic equations discussed earlier in Equations 1 and 2. In fact, if the applied normal force, *P*, is taken as zero, Equation 9 reduces to $M_n \approx \frac{2\sigma_T H^2}{9}$, which can be compared with the classic elastic distribution equation $\frac{\sigma_T H^2}{6}$ and the plastic distribution equation $\frac{\sigma_T H^2}{4}$.

In Tables 1 through 6, the *C* values calculated by applying Design Models 1 through 4 are compared to the corresponding *C* values in Table 8-4 of the AISC *Manual* (AISC, 2011). Note that, consistent with Table 8-4, the available strength values are calculated assuming no plate bearing occurs. The average percentage difference among the four models and the *C* values from the *Manual* are as follows: –31% for Model 1 (elastic), 6% for Model 2 (plastic), 0.1% for Model 3 (ICoR), and –3% for Model 4 (elliptical). Because Design Model 3 and Table 8-4 both use the ICoR method, it is not surprising that there is little difference between the predicted available strength values.

While the linear elastic method used for Design Model 1 is computationally easy and convenient for design, it is, on average, 31% conservative. Thus, the use of Design Model 1 could lead to larger fillet weld sizes than required, which can increase fabrication costs. However, Design Model 1 could be used by the designer to verify a lightly loaded connection boundary is adequate if the model does not dictate the use of a fillet weld larger than the minimum fillet weld size to be used on the project.

Design Model 2 assumes a uniform plastic stress distribution and predicts available strength values that are, on average, 6% greater than those presented in Table 8-4 of the AISC *Manual* (AISC, 2011). The primary reason for this

discrepancy is that Design Model 2 assumes that the full strength of the fillet weld can exist along the full length of the welded boundary. Assuming rigid-body rotation of the plate suggests that the welds along the extreme edges of the plate would experience the largest deformation demands in order to allow this stress to propagate along the length of the plate as the extreme ends plastically deform. This plastic deformation demand forms the basis of the ductility considerations previously discussed for Design Model 2. While the author knows of no experimental data that would give insight as to the measured stress distribution along the fillet-welded boundary of a connected plate, there is evidence that the ductility of fillet welds is affected by both the welding process and the specified weld toughness levels of the weld metal (Deng et. al, 2006). Given the variation in weld ductility, the author recommends that designers pay particular attention to ensuring ductility of the connection plate boundary when using Design Model 2.

Design Model 4 has been shown to give results similar to Design Model 3, within 3% on average, but it is not an iterative procedure. Rather than calculating the required weld size for the applied load, as in Design Model 1, the designer obtains the strength of the welded boundary using Equations 8 and 9 and then compares the strength to the applied eccentric shear. It is important to emphasize the preceding point to understand what the F_c force given in Equation 10 actually is—the compressive resultant bearing force that would exist at the point where the strength of the welded boundary is reached. The F_c force is not the actual bearing force in the connection under the applied loading.

Given the ductile nature of steel and the many ill-defined variables that affect the true stress state, it is generally considered acceptable practice to design the connection elements for the simple stresses resulting from the connection free-body diagram forces and moments; see Section 9 of the AISC *Manual* (AISC, 2011) for more discussion on this topic. Therefore, ensuring the available strength of the connection plate's boundary is adequate, rather than assessing the actual stress state in the connection element, is considered acceptable for daily design practice.

The only situation in which Design Model 4 will not be valid is if the neutral axis is calculated to be off of the plate—for example, if the axial load significantly dominates over the effect of the eccentric shear. To handle such a case, it is best to use Design Model 3, or if doing the design calculation by hand, then Design Models 1 or 2 should be used.

Comparison of Design Model 4 with Plate Bearing to Test Data

To verify the proposed Design Model 4 with plate bearing, a comparison is made with the test data presented by Kwan et al. (2010). The test data presented in the work by Kwan et al. reference three primary testing programs in establishing recommendations for a design model: Dawe and Kulak (1972), Beaulieu and Picard (1985), as well as the work conducted by Kwan et al. at UC Davis/University of Alberta. Equations 22 and 25 will be used to analyze the test data and the resulting comparison is given in Figures 11, 12 and 13 in the form of tested and predicted capacity graphs.

Of note, Equation 22 has been applied to the work of Dawe and Kulak (1972) because they recommended a triangular bearing stress distribution. However, a rectangular bearing stress distribution, Equation 25, is used for the comparison of the work by Kwan et al. (2010) and Beaulieu and Picard (1985), as recommended by Kwan et al. It should also be noted that Kwan et al. primarily presented two types of data—corresponding to specimens fabricated with weld-metal toughness requirements and those without—to reflect the observed influence of toughness on fillet weld ductility. To be as conservative as possible, the test data are presented only for those with no toughness rating; increased weld ductility would allow the design strength of the weld to propagate further along the length of the weld, thus resulting in a larger available strength.

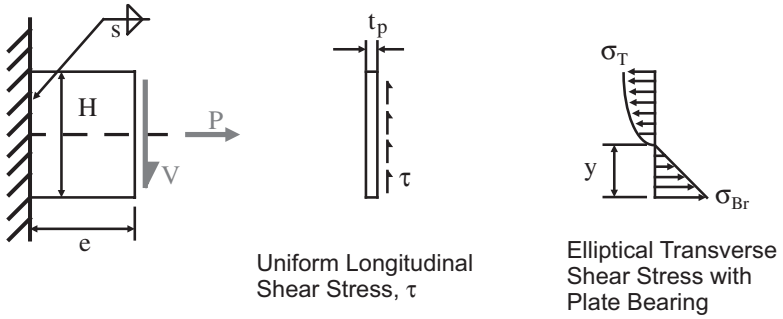

Fig. 10. Assumed stress distribution for Design Model 4—with plate bearing.

The average test-to-predicted ratio for the aforementioned test data is 1.20 with a coefficient of variation of 0.19. These values are compared with an average test-to-predicted ratio and coefficient of variation of 1.06 and 0.21, respectively, reported by Kwan et al. (2010)—using the ICoR approach with a rectangular stress distribution and the fillet weld response curves proposed by Lesik and Kennedy (1990). Kwan et al. report that this ICoR approach results in a suitable safety index for use with LRFD; a target of 4.0 is usually deemed appropriate for welded connections, and values

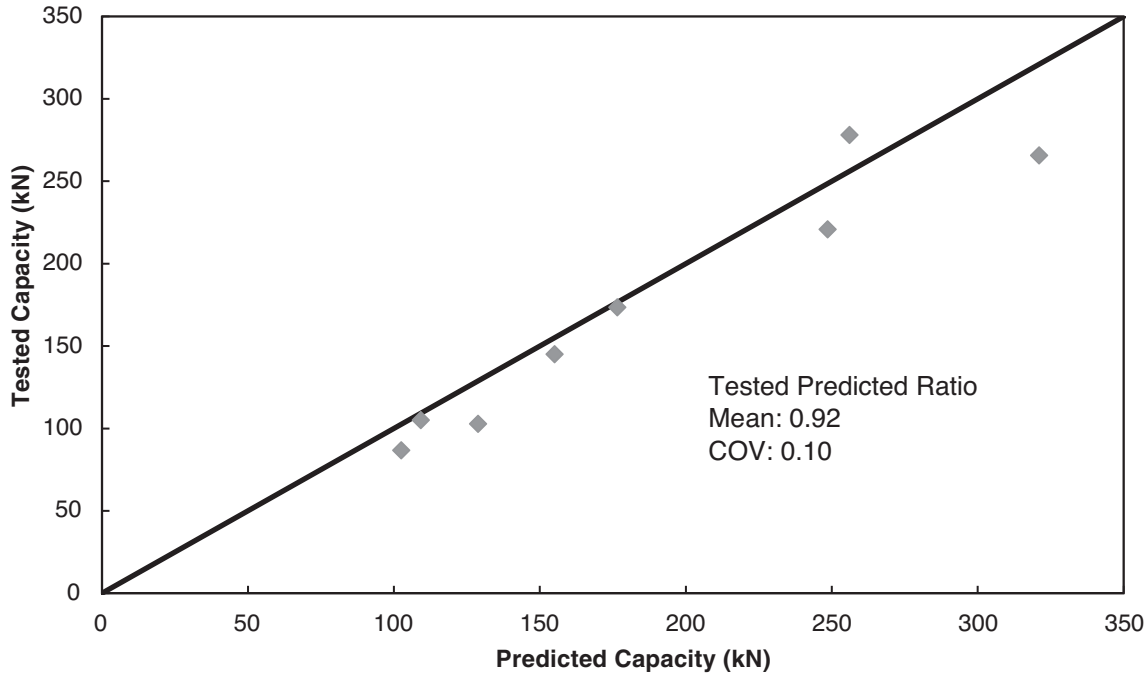

Fig. 11. Dawe and Kulak test-to-predicted ratios using Equation 22.

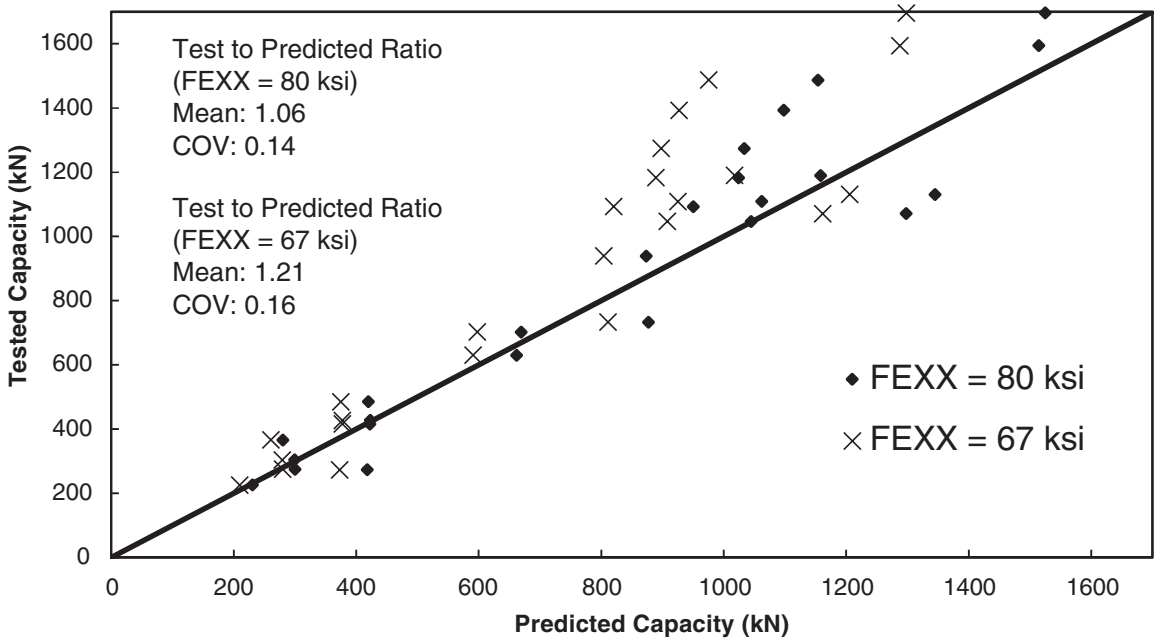

Fig. 12. Beaulieu and Picard test-to-predicted ratios using Equation 25.

between 4.0–4.5 are reported. Thus, because an analysis of the test data with Design Model 4 would result in a larger safety index and because the average test-to-predicted ratio is larger and the variance is smaller, the model is validated as having an acceptable safety index as well.

Even though Equations 22 and 25 have been shown to have an adequate level of safety to be used in design, they are still recommended for use only when the web strength or stability limit states are exceeded by the F_c force. The reason for this is that the referenced tests were all specifically fabricated with proper fit-up that ensured plate bearing occurred. During typical fabrication practice, there is a possibility of a gap between the connection plate and the flange of the W-shape because the plate must be fit to allow precise location of the bolt holes typically predrilled in the plate. The author's experiences in fabrication suggest that the size of the gap can commonly be up to approximately ⅛ in. Therefore, the use of Equation 9 is recommended, in general, as an upper bound to the available strength of the welded boundary because the presence of a gap does not violate any of the assumptions that went into the development of this equation.

The reason for using Equation 22 in Design Model 4, with its assumed triangular bearing stress distribution, is that the longest plate length tested was approximately 12 in. Connection plates can exceed 12 in. quite commonly in practice, and a longer plate length would require more deformation demand on the exterior portions of the weld in order to allow the plastic redistribution that must occur to obtain a rectangular bearing stress distribution. Until longer connection elements have been tested, it is recommended to use the more conservative Equation 22.

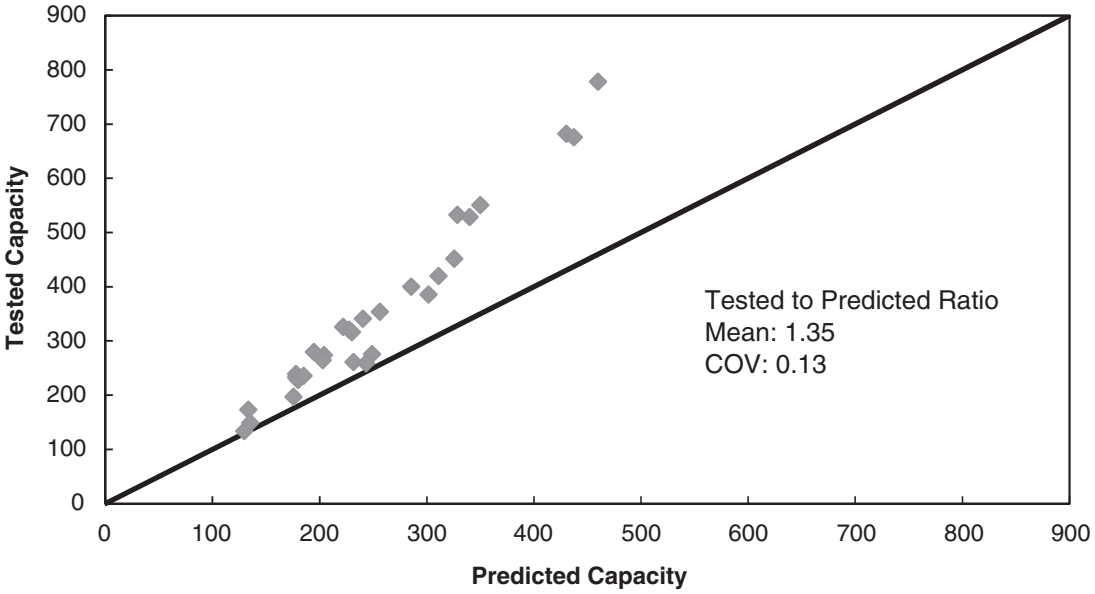

Fig. 13. UC Davis–Kwan et. al partial test-to-predicted ratios using Equation 25.

DESIGN EXAMPLE 1

Assess the axial load that will reach the design strength of an end plate using the proposed alternate fillet weld criteria shown in Figure 9 and described in Equation 15. The end plate used for this design example is shown in Figure 14. The sample calculation will be presented using the LRFD method only.

Given:

The W12 web thickness is assumed to be sufficient to avoid the web governing over the weld, and the weld length is assumed to be $2\left[9 \text{ in.} - (2)(\text{¼ in.})\right] = 17$ in. total to account for start/stop effects. The welds will be assumed to be made with E70XX electrodes.

Solution:

First, the value of N_L will be evaluated using Equation 17 with $\phi = 0.75$ applied in the denominator; then Equation 18 will be applied.

$$N_L = \frac{\tau}{0.6s\sqrt{2}F_{EXX}} \tag{17}$$

$$= \frac{\dfrac{30 \text{ kips}}{17 \text{ in.}/2}}{0.6(0.75)(\text{¼ in.})\left(\sqrt{2}\right)(70 \text{ ksi})}$$

$$= \frac{3.53 \text{ kip/in.}}{11.1 \text{ kip/in.}}$$

$$= 0.318$$

$$N_L < 1.0, \quad \therefore \tag{18}$$

$$N_T = 0.6 + 0.9\sqrt{1.0 - N_L^2}$$

$$= 0.6 + 0.9\sqrt{1.0 - 0.318^2}$$

$$= 1.45$$

The maximum factored axial force, P_{max}, that can be applied to the beam that would result in the end plate weld reaching its design strength can now be calculated using Equation 19 with $\phi = 0.75$.

$$\sigma_T = 0.6\sqrt{2}sF_{EXX}N_T$$

$$P_{max} = 0.6(0.75)(\text{¼ in.})\left(\sqrt{2}\right)\left(\frac{17 \text{ in.}}{2}\right)(70 \text{ ksi})(1.45)$$

$$= 137 \text{ kips} \tag{19}$$

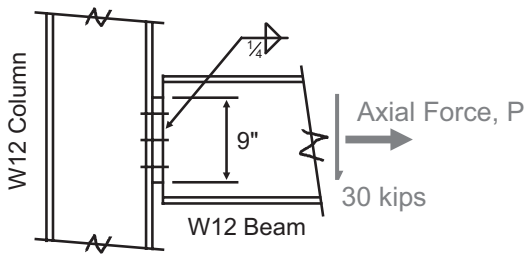

Fig. 14. Design Example 1—design the end plate weld.

For comparison, the vector summation of the forces (141 kips) is seen to be within 1 kip of the AISC *Specification* equation, as shown here:

$$\sqrt{30^2 + 137^2} = 140 \text{ kips} \qquad \text{(AISC } \textit{Specification} \text{ J2-4)}$$

$$\tan\theta = \frac{137 \text{ kips}}{30 \text{ kips}} \qquad \theta = 78°$$

$$\phi V_n = 0.6(0.75)(¼ \text{ in.})\left(\sqrt{2}\right)\left(\frac{17 \text{ in.}}{2}\right)(70 \text{ ksi})(1.0 + 0.5\sin^{1.5} 78°)$$

$$= 141 \text{ kips}$$

DESIGN EXAMPLE 2

Assess the welded boundary of the gusset plate shown in Figure 15 to illustrate the application of Design Model 4. The sample calculation will be presented using the LRFD method only.

Given:

The gusset plate material will be assumed to be ASTM A36, while the W12×30 beam will be assumed to be from ASTM A992 Grade 50. The welds will be assumed to be made with E70XX electrodes. The braces are assumed to be L5×5×0.375 angles with three 1-in.-diameter A325 bolts on each end of the brace, resulting in a gusset plate length, *L*, of 32 in. The applied factored loads are as given in Figure 15.

Solution:

First, the internal forces on the gusset boundary—*N*, *S* and *M*—are calculated by applying the three equations of statics to a free-body diagram of the gusset. It is seen that $N = 50$ kips, $S = 142$ kips, and $M = (S)(e) = (142 \text{ kips})(12.3 \text{ in.}/2) = 873$ kip-in. Note that both brace forces and the 50-kip force from the post above is assumed to occur at the same time, resulting in total brace forces of 135 kips (compression) and 65 kips (tension).

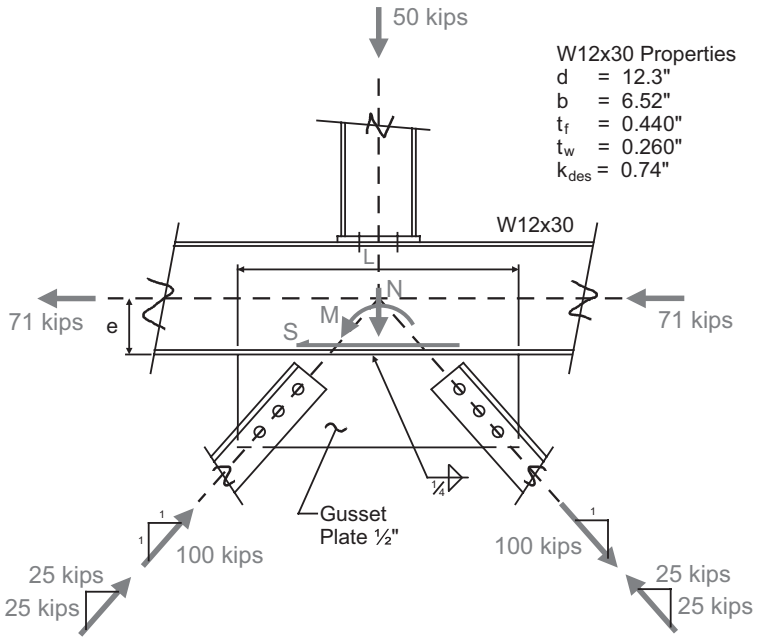

Fig. 15. Design Example 2—gusset weld connection example.

Applying Equations 7 and 17–19, with $\phi = 0.75$, to calculate σ_T:

$$\tau = \frac{S}{L} \quad \text{(from Eq. 7)}$$
$$= \frac{142 \text{ kips}}{32 \text{ in.}}$$
$$= 4.44 \text{ kip/in.}$$

$$N_L = \frac{\tau}{0.6\phi s\sqrt{2}F_{EXX}} \quad (17)$$
$$= \frac{4.44 \text{ kip/in.}}{0.6(0.75)(¼ \text{ in.})\left(\sqrt{2}\right)(70 \text{ ksi})}$$
$$= 0.400$$

$$N_T = 0.6 + 0.9\sqrt{1.0 - N_L^2} \quad (18)$$
$$= 0.6 + 0.9\sqrt{1.0 - (0.400)^2}$$
$$= 1.43$$

$$\sigma_T = 0.6\phi\sqrt{2}sF_{EXX}N_T \quad (19)$$
$$= 0.6(0.75)\sqrt{2}(¼ \text{ in.})(70 \text{ ksi})(1.43)$$
$$= 15.9 \text{ kip/in.}$$

Note that the ½-in. A36 plate can transfer the σ_T stress: $\phi F_{yt} = 0.90(36 \text{ ksi})(½ \text{ in.}) = 16.2$ kip/in. With σ_T calculated, the neutral axis position and design strength of the fillet-welded gusset plate boundary are evaluated using Equations 8 and 9.

$$y = \frac{L}{2} - \frac{2P}{\pi\sigma_T} \quad (26)$$
$$= \frac{32 \text{ in.}}{2} - \frac{2(-50 \text{ kips})}{\pi(15.9 \text{ kip/in.})}$$
$$= 18.0 \text{ in.}$$

$$\phi M_n = \sigma_T\left(\frac{\pi}{4} - \frac{1}{3}\right)\left[y^2 + (L-y)^2\right] - (-N)\left(\frac{L}{2} - y\right) \quad (27)$$
$$= 15.9 \text{ kip/in.}\left(\frac{\pi}{4} - \frac{1}{3}\right)\left[(18 \text{ in.})^2 + (32 \text{ in.} - 18 \text{ in.})^2\right] + 50 \text{ kips}\left(\frac{32 \text{ in.}}{2} - 18 \text{ in.}\right)$$
$$= 3{,}640 \text{ kip-in.}$$

With reference to Figures 2 and 15, note that the normal force, N, from Design Example 2 is acting in the opposite direction to the axial force, P, in Figure 2; thus, a value of –50 kips is applied in Equation 26. Because $\phi M_n \geq M$, 3,630 kip-in >> 873 kip-in, the weld strength is adequate. However, the load path assumed by Design Model 4 must be followed, and the local web strength and crippling checks still need to be performed to ensure that the local web limit states would not affect the design strength of the connection boundary.

As previously discussed, the author emphasizes that in the following checks, the beam web is not actually subjected to the F_c force shown in Equation 28 because this is the compressive force that would be mobilized by the weld at its ultimate strength. The reason this fictitious compressive force is used is to be consistent with the stress distribution assumed for the weld. Thus, instead of checking the web against the stresses from the applied loads, the web will be assessed to see if it would limit the weld's design strength; if so, then weld's design strength will be calculated using Equation 22.

By applying Equation 10, the magnitude of the compressive force in the assumed elliptical stress block, F_c, is calculated as:

$$F_c = \frac{\pi}{4}(\sigma_T y) \tag{28}$$
$$= \frac{\pi}{4}(15.9\,\text{kip/in.})(18\text{ in.})$$
$$= 225\text{ kips}$$

The web local yield strength, as given by Equation J10-2 of the Specification, which governs over the gusset plate bearing, is calculated in Equation 29. The F_c force is seen to be less than the web local yield strength; thus, this limit state will not necessitate a reduction in the design strength of the welded boundary.

$$\phi R_n = \phi F_{yw} t_w (5k + l_b) \tag{29}$$
$$= 1.0(50\text{ ksi})(0.26\text{ in.})\left[(5)(0.74\text{ in.}) + 15.3\text{ in.}\right]$$
$$= 247\text{ kips}$$

In order to ensure that the uniform stress resistance that is represented by Equation 29 is centered about the centroid of the quarter ellipse assumed stress distribution, the bearing length, l_b, in Equation 29 is calculated using Equation 20: $2\left(\frac{4y}{3\pi}\right) = 15.3$ in.; see Figure 16.

In the interest of brevity, the local web crippling and stability will be assessed by applying only Equation J104 of the AISC *Specification* (AISC, 2010), given in Equation 30. If the W12×30 beam was not laterally supported at the connection location, then Section J10.4 would have to be considered. Consideration should also be given to the overall stability of the web using an analysis similar to that presented in Section J10.5 of the AISC *Specification* because the post likely provides enough compression to the web that it is reasonable, though admittedly conservative, to apply Equation J10-8 of the AISC *Specification*.

$$\phi R_n = \phi 0.80 t_w^2 \left[1 + 3\left(\frac{l_b}{d}\right)\left(\frac{t_w}{t_f}\right)^{1.5}\right]\sqrt{\frac{EF_{yw}t_f}{t_w}} \tag{30}$$
$$= 0.75(0.80)(0.26\text{ in.})^2\left[1 + 3\left(\frac{15.3\text{ in.}}{12.3\text{ in.}}\right)\left(\frac{0.26\text{ in.}}{0.44\text{ in.}}\right)^{1.5}\right]\sqrt{\frac{29{,}000\,\text{ksi}(50\text{ ksi})(0.44\text{ in.})}{0.26\text{ in.}}}$$
$$= 171\text{ kips}$$

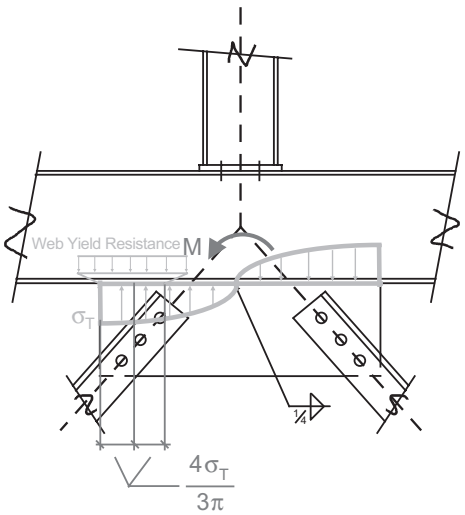

Fig. 16. Design Example 2—web bearing length for compressive check.

Because the local web crippling design strength of 170 kips is less than the F_c force of 225 kips, the design strength of the weld will be adjusted using Equation 22 because the web would undergo local crippling prior to the weld reaching the assumed stress distribution. The compressive force from the assumed stress distribution on the fillet weld must be limited to 170 kips to ensure that the web crippling will not govern. Thus, applying Equation 23 to calculate σ_{Br}, a new design strength can be calculated using Equations 21 and 22.

$$\begin{aligned}\sigma_{Br} &= \phi F_{yw} t_w \\ &= 1.0(50\text{ ksi})(0.26\text{ in.}) \\ &= 13.0\text{ kip/in.}\end{aligned} \tag{23}$$

$$\begin{aligned}y &= \frac{\frac{\pi}{4}(\sigma_T L) - (-N)}{\frac{\pi}{4}\sigma_T + \frac{\sigma_{Br}}{2}} \\ &= \frac{\frac{\pi}{4}(15.9\text{ kip/in.})(32\text{ in.}) + 50\text{ kips}}{\frac{\pi}{4}(15.9\text{ kip/in.}) + \frac{13\text{ kip/in.}}{2}} \\ &= 23.7\text{ in.}\end{aligned} \tag{21}$$

$$\begin{aligned}\phi M_n &= \sigma_T\left(\frac{\pi}{4} - \frac{1}{3}\right)(L-y)^2 + \frac{\sigma_{Br} y^2}{3} - (-N)\left(\frac{L}{2} - y\right) \\ &= 15.9\,\text{kip/in.}\left(\frac{\pi}{4} - \frac{1}{3}\right)(32\,\text{in.} - 23.7\,\text{in.})^2 + \frac{13\,\text{kip/in.}\,(23.7\,\text{in.})^2}{3} + 50\text{ kips}\left(\frac{32\text{ in.}}{2} - 23.7\,\text{in.}\right) \\ &= 2{,}540\text{ kip-in.}\end{aligned} \tag{22}$$

Here we see that the design strength of the boundary is less than that calculated in Equation 27 because local web crippling limited the design strength; however, because $\phi M_n \geq M$, the design strength of the welded boundary is adequate to resist the applied loads. The magnitude of the resultant compressive force from the triangular bearing stress distribution is $\frac{1}{2} y \sigma_{Br} = \frac{1}{2}$(23.7 in.)(13 kip/in.) = 154 kips, which is less than 170 kips; thus, the local web crippling limit state has also been satisfied.

Design checks are complete for the welded boundary of the gusset plate shown in Figure 15.

SUMMARY

Given both the favorable qualitative and quantitative comparisons between Design Model 4 and the other design models (see Tables 1 through 6 and Figures 5 and 11 through 14), it is proposed that Design Model 4 can now be used in design applications. Equations 7, 9 and 19 provide the designer with a flexible direct solution that can quickly and easily handle nearly all design scenarios. Further, Design Model 4 allows the designer to directly follow the assumed load path to assess any local web strength or stability limit states if the connection plate is welded to a W-shape member's flange.

By ensuring that the ultimate strength of the fillet welds is only counted on at the extreme edges of the plate and assuming an elliptical stress distribution, Design Model 4 also indirectly accounts for the load-deformation and ductility characteristics of fillet welds. These considerations are necessary in applying the lower bound theorem often used in connection design; see AISC Design Guide 29 (Muir and Thornton, 2014) for a good discussion on this topic.

The ability to directly follow the assumed load path and ensure that the assumed stresses are within acceptable limits across the entire connection boundary is the primary merit of the proposed method. And given the importance of safe and efficient design of connection components (such as the one presented herein) for successful structural steel construction projects, the author hopes that designers will find the information presented useful in structural steel connection design.

TABLE 1. Comparison of Design Methods with No Applied Normal Force					
Eccentric Weld Group Coefficient, *C*; Load Angle = 0°					
		Design Model Number			
a	AISC Manual*	1	2	3	4
0.3	3.090	2.608	3.271	3.125	3.121
0.4	2.660	2.108	2.813	2.686	2.637
0.5	2.300	1.750	2.422	2.310	2.246
0.6	2.000	1.490	2.108	2.005	1.941
0.7	1.760	1.294	1.857	1.763	1.703
0.8	1.570	1.142	1.654	1.567	1.513
0.9	1.410	1.021	1.490	1.409	1.359
1.0	1.280	0.923	1.353	1.278	1.232
1.2	1.080	0.773	1.142	1.075	1.038
1.4	0.928	0.665	0.986	0.927	0.895
1.6	0.815	0.583	0.867	0.814	0.786
1.8	0.727	0.519	0.773	0.725	0.701
2.0	0.655	0.468	0.698	0.654	0.632
2.2	0.597	0.426	0.635	0.595	0.575
2.4	0.547	0.390	0.583	0.546	0.528
2.6	0.506	0.361	0.539	0.504	0.488
2.8	0.470	0.335	0.501	0.469	0.453
3.0	0.439	0.313	0.468	0.438	0.423
Average % difference:		–26.7%	6.0%	0.0%	–3.1%

* Table 8-4, *Steel Construction Manual* (AISC, 2011).

TABLE 2. Comparison of Design Methods with Resultant Applied Force at a 15° Incline from the Welded Boundary					
Eccentric Weld Group Coefficient, *C*; Load Angle = 15°					
		Design Model Number			
a	AISC Manual*	1	2	3	4
0.3	3.090	2.410	3.267	3.135	3.109
0.4	2.680	1.971	2.821	2.705	2.642
0.5	2.320	1.656	2.438	2.336	2.261
0.6	2.030	1.423	2.128	2.036	1.960
0.7	1.790	1.245	1.879	1.795	1.723
0.8	1.600	1.106	1.677	1.600	1.533
0.9	1.440	0.994	1.511	1.441	1.379
1.0	1.310	0.902	1.374	1.309	1.252
1.2	1.110	0.761	1.161	1.104	1.055
1.4	0.954	0.658	1.003	0.953	0.911
1.6	0.839	0.579	0.883	0.838	0.800
1.8	0.748	0.517	0.787	0.747	0.714
2.0	0.675	0.467	0.711	0.674	0.644
2.2	0.615	0.425	0.647	0.614	0.586
2.4	0.565	0.391	0.594	0.563	0.538
2.6	0.522	0.361	0.549	0.520	0.497
2.8	0.485	0.336	0.510	0.484	0.462
3.0	0.453	0.314	0.477	0.452	0.431
Average % difference:		–30.0%	5.1%	0.1%	–3.9%
* Table 8-4, *Steel Construction Manual* (AISC, 2011).					

TABLE 3. Comparison of Design Methods with Resultant Applied Force at a 30° Incline from the Welded Boundary					
Eccentric Weld Group Coefficient, *C*; Load Angle = 30°					
		Design Model Number			
a	AISC Manual*	1	2	3	4
0.3	3.220	2.415	3.411	3.268	3.225
0.4	2.810	2.004	2.981	2.845	2.783
0.5	2.460	1.704	2.607	2.482	2.413
0.6	2.170	1.479	2.296	2.181	2.113
0.7	1.930	1.304	2.041	1.936	1.871
0.8	1.730	1.166	1.831	1.735	1.674
0.9	1.570	1.053	1.657	1.568	1.511
1.0	1.430	0.960	1.511	1.429	1.376
1.2	1.210	0.816	1.281	1.211	1.165
1.4	1.050	0.709	1.110	1.049	1.008
1.6	0.926	0.626	0.978	0.924	0.887
1.8	0.827	0.561	0.874	0.826	0.792
2.0	0.747	0.508	0.789	0.746	0.715
2.2	0.681	0.464	0.720	0.680	0.652
2.4	0.626	0.427	0.661	0.624	0.598
2.6	0.579	0.395	0.611	0.577	0.553
2.8	0.538	0.368	0.568	0.537	0.514
3.0	0.503	0.345	0.531	0.502	0.480
Average % difference:		–31.5%	5.7%	0.2%	–3.4%

* Table 8-4, *Steel Construction Manual* (AISC, 2011).

TABLE 4. Comparison of Design Methods with Resultant Applied Force at a 45° Incline from the Welded Boundary					
Eccentric Weld Group Coefficient, *C*; Load Angle = 45°					
		Design Model Number			
a	AISC Manual*	1	2	3	4
0.3	3.490	2.586	3.679	3.539	3.445
0.4	3.100	2.184	3.277	3.132	3.045
0.5	2.750	1.885	2.922	2.778	2.699
0.6	2.460	1.655	2.616	2.477	2.406
0.7	2.210	1.474	2.356	2.225	2.159
0.8	2.010	1.328	2.136	2.013	1.952
0.9	1.830	1.208	1.948	1.834	1.777
1.0	1.680	1.107	1.788	1.682	1.629
1.2	1.440	0.949	1.530	1.438	1.391
1.4	1.250	0.829	1.334	1.254	1.211
1.6	1.110	0.737	1.180	1.109	1.071
1.8	0.996	0.663	1.058	0.994	0.959
2.0	0.902	0.602	0.957	0.900	0.867
2.2	0.824	0.551	0.874	0.822	0.792
2.4	0.758	0.509	0.804	0.756	0.728
2.6	0.702	0.472	0.744	0.700	0.674
2.8	0.653	0.440	0.692	0.652	0.627
3.0	0.611	0.413	0.647	0.610	0.586
Average % difference:		–32.6%	6.2%	0.2%	–3.1%
* Table 8-4, *Steel Construction Manual* (AISC, 2011).					

TABLE 5. Comparison of Design Methods with Resultant Applied Force at a 60° Incline from the Welded Boundary					
Eccentric Weld Group Coefficient, *C*; Load Angle = 60°					
		Design Model Number			
a	AISC Manual*	1	2	3	4
0.3	3.930	2.985	4.107	3.966	3.806
0.4	3.580	2.587	3.762	3.606	3.473
0.5	3.260	2.279	3.448	3.285	3.173
0.6	2.980	2.035	3.166	3.001	2.906
0.7	2.740	1.838	2.915	2.752	2.669
0.8	2.520	1.674	2.692	2.534	2.460
0.9	2.340	1.537	2.494	2.343	2.276
1.0	2.170	1.421	2.319	2.175	2.114
1.2	1.890	1.233	2.025	1.895	1.843
1.4	1.667	1.089	1.791	1.675	1.627
1.6	1.500	0.975	1.601	1.497	1.454
1.8	1.350	0.883	1.446	1.352	1.311
2.0	1.230	0.806	1.316	1.231	1.193
2.2	1.130	0.742	1.207	1.129	1.094
2.4	1.040	0.687	1.114	1.043	1.009
2.6	0.970	0.640	1.034	0.968	0.936
2.8	0.905	0.598	0.964	0.903	0.873
3.0	0.848	0.562	0.903	0.847	0.818
Average % difference:		–32.9%	6.5%	0.3%	–2.9%
* Table 8-4, *Steel Construction Manual* (AISC, 2011).					

TABLE 6. Comparison of Design Methods with Resultant Applied Force at a 75° Incline from the Welded Boundary					
Eccentric Weld Group Coefficient, *C*; Load Angle = 75°					
		Design Model Number			
a	AISC Manual*	1	2	3	4
0.3	4.570	3.796	4.734	4.558	4.347
0.4	4.320	3.438	4.507	4.317	4.133
0.5	4.090	3.141	4.291	4.095	3.931
0.6	3.880	2.891	4.087	3.888	3.741
0.7	3.690	2.677	3.895	3.694	3.561
0.8	3.510	2.492	3.714	3.513	3.393
0.9	3.340	2.331	3.544	3.343	3.235
1.0	3.180	2.190	3.384	3.186	3.087
1.2	2.900	1.952	3.095	2.903	2.820
1.4	2.650	1.761	2.840	2.657	2.585
1.6	2.440	1.604	2.618	2.443	2.380
1.8	2.260	1.472	2.422	2.257	2.201
2.0	2.090	1.361	2.249	2.094	2.043
2.2	1.950	1.265	2.097	1.951	1.903
2.4	1.820	1.181	1.961	1.825	1.779
2.6	1.710	1.108	1.841	1.712	1.669
2.8	1.610	1.044	1.733	1.612	1.571
3.0	1.520	0.986	1.636	1.522	1.483
Average % difference:		–30.5%	6.5%	0.1%	–3.0%
* Table 8-4, *Steel Construction Manual* (AISC, 2011).					

SYMBOLS

F_c Magnitude of the resultant compressive force from the assumed elliptical stress distribution, see Figure 8, (kips)

H Length of the connection plate under consideration, see Figure 2, (in.)

M_n Nominal strength of the fillet-welded boundary under an eccentric shear, V, (kip-in.)

N_L Nondimensional longitudinal weld factor, the ratio of V_{nL} to the nominal weld strength with no strength increase provided as a function of θ, i.e., $V_{nL}/0.6A_wF_{EXX}$

N_T Nondimensional transverse weld factor, the ratio of V_{nT} to the nominal weld strength with no strength increase provided as a function of θ, i.e., $V_{nT}/0.6A_wF_{EXX}$

P Applied concentric tensile force to the connection plate under consideration, see Figure 2, (kips)

V Applied eccentric shear force to the connection plate under consideration, see Figure 2, (kips)

V_n Vector nominal strength of the fillet weld, (kips)

V_{nL} Longitudinal shear component of the applied load if the applied load matches the nominal strength, (kips)

V_{nT} Transverse shear component of the applied load if the applied load matches the nominal strength, (kips)

e Eccentricity of the shear as measured out from the connection boundary, see Figure 2, (in.)

s Size of the fillet weld on both sides of the connection plate under consideration, see Figure 2, (in.)

t_p Thickness of the connection plate under consideration, see Figure 2, (in.)

y Distance to the neutral axis measured from the compression edge of the plate, see Figure 7, (in.)

Δ_{ult} Fillet weld deformation, measured in the direction of the applied load, at the point where the fillet weld reaches it nominal (ultimate) strength, (in.)

τ Assumed uniform shear stress on the connection plate boundary, (kip/in.)

σ_M Maximum stress used in linear elastic stress distribution assumed in Design Model 1, $\sigma_M \le F_{yp} \times t_p$, (kip/in.)

σ_P Stress used in plastic stress distribution assumed in Design Model 2, (kip/in.)

σ_T Maximum fillet weld transverse shear stress on fillet weld s used in Design Model 4, (kip/in.)

σ_{Br} Maximum bearing stress used in Design Model 4, equal to $F_{yw} \times t_w$ when local web yield or crippling is checked and equal to $F_{yp} \times t_p$ when assessing the experimental data discussed herein, (kip/in.)

θ Weld orientation between line of action of the applied load and long axis of the fillet weld; a longitudinal fillet weld is orientated such that $\theta = 0°$ and a transverse fillet weld has $\theta = 90°$, (degrees)

APPENDIX A
DETAILED DERIVATION OF EQUATIONS 8 AND 9

With reference to Figure 8 and Equation 10, as well as the established geometric properties of an ellipse, Equations 8 and 9 can be derived by equating the internal stress distribution with the external applied loads and summing moments about the neutral axis.

With reference to the compressive portion of the assumed quarter ellipse stress distribution, the compressive force, F_c, is as given in Equation A1 and Equation 10. Similarly, the tensile force, F_t, is as given in Equation A2.

$$F_c = \frac{\pi}{4}(\sigma_T y) \tag{A1}$$

$$F_t = \frac{\pi}{4}\sigma_T (H - y) \tag{A2}$$

Now equating the difference between Equations A1 and A2 with the applied load, P, to establish horizontal equilibrium, Equation 8 is obtained as follows:

$$\frac{\pi}{4}\sigma_T \left[(H - y) - y\right] = P$$

$$H - 2y = \frac{4P}{\pi\sigma_T}$$

$$y = \frac{H}{2} - \frac{2P}{\pi\sigma_T}$$

Again using the properties of an ellipse, the location of the two resultant forces, F_c and F_t, can be calculated as follows:

$$d_c = \frac{4y}{3\pi} \tag{A3}$$

$$d_t = \frac{4(H - y)}{3\pi} \tag{A4}$$

Then, summing moments about the neutral axis and equilibrating the internal moment with the external moments from the eccentric shear and axial load, we get the following:

$$F_c(y-d_c)+F_t(H-y-d_t)=Ve+P\left(\frac{H}{2}-y\right) \quad \text{(A5)}$$

Now substituting Equations A1 through A4 into Equation A5, the value for *Ve* is obtained:

$$\begin{aligned}Ve &= \frac{\pi}{4}(\sigma_T y)\left(y-\frac{4y}{3\pi}\right)+\frac{\pi}{4}\sigma_T(H-y)\left[H-y-\frac{4(H-y)}{3\pi}\right] \\ &\quad -P\left(\frac{H}{2}-y\right) \\ &= \frac{\pi}{4}(\sigma_T)\left[y^2\left(1-\frac{4}{3\pi}\right)+(H-y)^2\left(1-\frac{4}{3\pi}\right)\right]-P\left(\frac{H}{2}-y\right) \\ &= \left(1-\frac{4}{3\pi}\right)\left(\frac{\pi}{4}\right)(\sigma_T)\left[y^2+(H-y)^2\right]-P\left(\frac{H}{2}-y\right) \\ &= \left(\frac{\pi}{4}-\frac{1}{3}\right)(\sigma_T)\left[y^2+(H-y)^2\right]-P\left(\frac{H}{2}-y\right)\end{aligned}$$

Thus, the nominal strength of the welded boundary presented in Equation 9 is obtained.

REFERENCES

AISC (2010), *Specification for Structural Steel Buildings*, ANSI/AISC 360-10, American Institute of Steel Construction, Chicago, IL.

AISC (2011), *Steel Construction Manual*, 14th Ed., American Institute of Steel Construction, Chicago, IL.

Beaulieu, D. and Picard, A. (1985), "Résultats d'essais sur des assemblages soudés excentriques en flexion," *Canadian Journal of Civil Engineering*, Vol. 12, pp. 494–506.

Blodgett, O.W. (1966), *Design of Welded Structures*, Chapter 5, James F. Lincoln Foundation.

Butler, L.J., Pal, S. and Kulak, G.L. (1972), "Eccentrically Loaded Welded Connections," *ASCE Journal of the Structural Division*, Vol. 98, No. ST5.

Callele L.J., Driver, R.G. and Grondin, G.Y. (2009), "Design and Behavior of Multi-Orientation Fillet Weld Connections," *Engineering Journal,* AISC, Vol. 46, No. 4.

Dawe, J.L. and Kulak, G.L. (1974), "Welded Connections under Combined Shear and Moment," *ASCE Journal of the Structural Division*, Vol. 100, No. St4, pp. 727–741.

Deng K., Driver R.G. and Grondin G.Y. (2006), "Effect of Loading Angle on the Behavior of Fillet Welds," *Engineering Journal,* AISC, Vol. 43, No. 1, pp. 9–24.

Hewitt C.M. and Thornton W.A. (2004), "Rationale behind and Proper Application of the Ductility Factor for Bracing Connections Subjected to Shear and Transverse Loading," *Engineering Journal,* AISC, Vol. 41, No. 1.

Kwan Y.K., Gomez I.R., Grondin G.Y. and Kanvinde A.M. (2010), "Strength of Welded Joints under Combined Shear and Out-of-Plane Bending," *Canadian Journal of Civil Engineering*, Vol. 37, No. 2, pp. 250–261.

Lesik, D.F. and Kennedy, D.J.L. (1990), "Ultimate Strength of Fillet Welded Connections Loaded in Plane," *Canadian Journal of Civil Engineering*, Vol. 17, No. 1, pp. 55–67.

Muir, L.S. and Thornton, W.A. (2014), *Vertical Bracing Connections—Analysis and Design*, Design Guide 29, American Institute of Steel Construction, Chicago, IL.